Published by
NIGERIAN SOCIETY OF PHYSICAL SCIENCES
Available online @ https://asr.nsps.org.ng/index.php/asr

African Scientific Reports 3 (2024) 247

African Scientific Reports

Simulation of thermochemical effects on unsteady magneto hydrodynamics fluids flow in two dimensional nonlinear permeable media

Solomon Denen Igba*, Idugba Mathias Echi, Emmanuel Vezua Tikyaa

Department of Physics, College of Physical Sciences, Joseph Sarwuan Tarkaa University Makurdi, Benue State, Nigeria

Abstract

This study aimed to simulate the thermochemical effects on unsteady magnetohydrodynamic (MHD) fluid flow in a two-dimensional nonlinear permeable medium under the influence of an external space-dependent magnetic field and a non-uniform heat source. Fluid flow is crucial in numerous natural and man-made systems, yet its complexities, especially in MHD contexts, are underexplored. The models momentum, energy, and concentration equations, accounting for the dependence of fluid and media properties, were transformed into nonlinear coupled ordinary differential equations using similarity transformations. These equations were solved numerically using the shooting technique, the sixth-order Runge-Kutta Fehlberg method, and Newton-Raphson method, supported by Maple software. Computational results were generated for velocity, temperature, and concentration profiles. The skin-friction coefficient, Nusselt Number (which represents heat transfer rate), and Sherwood Number (indicating mass transfer) were also evaluated. The results indicated that velocity increased with the magnetic field parameter, permeability, thermal and mass Grashof Numbers, Prandtl Number, radiation, mass transfer parameters, and wall porosity. Conversely, velocity diminished with an increase in Schmidt Number, space and temperature-dependent heat generation parameters, and unsteadiness. The fluid temperature followed a similar trend, decreasing with increased magnetic field, permeability, Grashof numbers, and other parameters but showed a reverse effect when radiation and unsteadiness were high. Fluid concentration initially increased with smaller parameter values but declined with larger ones. The findings suggested that optimizing thermophysical parameters can significantly enhance heat and mass transfer in unsteady MHD flow through permeable surfaces, making the results relevant for biomedical applications.

DOI:10.46481/asr.2024.3.3.247

Keywords: MHD fluids flow, Unsteady flow, Magnetic field, Similarity transformation, Heat and mass transfer

Article History :
Received: 07 October 2024
Received in revised form: 22 November 2024
Accepted for publication: 28 November 2024
Published: 30 December 2024

© 2024 The Author(s). Published by the Nigerian Society of Physical Sciences under the terms of the Creative Commons Attribution 4.0 International license. Further distribution of this work must maintain attribution to the author(s) and the published article's title, journal citation, and DOI.

1. Introduction

Fluid flow is vital in various natural phenomena and engineered systems, including the life cycles of stars, atmospheric formation, and energy production. Magnetohydrodynamic (MHD) flows, which involve the movement of magnetized electrically conducting fluids, have gained significance in multiple disciplines such as engineering, technology, astrophysics, geophysics, and nuclear science. These flows, characterized by heat and mass transfer, are observed in diverse environments, including the atmosphere, bodies of

*Corresponding author: Tel. No.: +234-810-923-9449.
Email address: denensolomon41@gmail.com (Solomon Denen Igba)

water, and quasi-solid materials [1]. In industrial applications, MHD effects are often utilized to address complex challenges, such as designing liquid metal blankets for thermonuclear fusion-fission hybrid reactors in nuclear engineering. Nonlinear permeable media also hold considerable value in academic, industrial, and medical fields, with applications in processes like transportation, glass-blowing, plastic sheet extraction, and hot rolling. Research is increasingly focused on nonlinear effects found in various materials, including gases, liquids, and solids. Examples of these nonlinear phenomena include nonlinear photo-absorption, harmonic generation, frequency mixing, self-focusing, nonlinear photoionization, photo-dissociation, and phase conjugation. Such nonlinear effects can significantly alter temperature distributions within fluid masses, influencing particle deposition rates and finding applications in biomedical devices, nuclear reactors, electronic chips, and semiconductor wafers [2, 3]. Fluids move through media, carrying heat and chemicals to different regions. The volume of fluid at open boundaries is determined by changes in temperature, concentration, and pressure, while the cross-sectional area is typically infinitesimally small [4]. Models of (MHD) fluid flow with functional dependency are more realistic, although they are frequently avoided due to the complexity and nonlinearity of the governing equations [5, 6]. Numerical approximation is a starting point for developing solutions using computer programming to investigate heat transmission and chemical reaction behavior in media. This study intends to model the thermochemical consequences of unsteady MHD fluid flow in 2D nonlinear permeable medium with an external magnetic field intensity and a non-uniform heat source. The research focuses on creating nonlinear mathematical models, developing numerical methods, analyzing heat transmission and mass transfer and investigating thermochemical parameters. Magneto hydrodynamics (MHD) is important in engineering, notably in micro Electrochemical Systems (MEMS), for applications like as quick mixing of biological fluids, biological transportation, and medication delivery. It generates a Lorentz force, which regulates electrically conducting fluid flow [7, 8]. In medical science, it is employed in transport processes such as the lungs, kidneys, gall bladders, arteries, and small blood vessels. Medical surgeons, radiologists, and researchers may be interested in the study's conclusions for managing blood flow during surgery, decreasing electromagnetic radiation, and evaluating the accuracy of theoretical works. The study aims to investigate the thermochemical effects on unsteady MHD flows in a permeable media, considering the effects of heat and mass transfer on MHD fluids flow. This study aims to advance the understanding of magnetohydrodynamic (MHD) fluid flow in nonlinear permeable media, which is crucial for optimizing fluid dynamics in applications with specific requirements for flow and heat transfer. Modeling MHD flow in a nonlinear permeable medium has significant relevance in biomedical applications such as targeted drug delivery systems, where magnetic fields control the movement of therapeutic agents and in industrial settings, where controlled heat and mass transfer are essential for system stability. This work focuses on how magnetic and thermal gradients influence fluid properties in permeable media, aiming to fill a gap in existing research regarding unsteady, nonlinear MHD flows.

In media, pipes are not explicit that can be used for measurements. The fine capillary like veins or pores through which the fluid flows are not of any uniform cross-section nor can they be said to be rigid. The consequence is that the flow parameters of media and fluids such as permeability of the media, viscosity, thermal diffusivity and mass diffusivity of fluid will depend on the momentum, temperature, concentration, pressure etc. [9]. In recent time, there is high level of cardiac attack which is attributed to atherosclerosis. The models of MHD fluids flow incorporating functional dependence of fluid and media properties are practically more realistic but are often avoided in the literature due to the complexity and nonlinearity of the media and governing equations. In some attempts, where nonlinearity is retained in the models, they are indirectly avoided at the solution stage through the process of linearization. This is like abandoning the problem at hand to pursue the ghost of it.

A research analysis on the effects of chemical reaction on unsteady MHD free convective two immiscible fluid flow was studied [10]. The results found out that the increase in chemical reaction coefficients or parameter suppresses both velocity and concentration profiles respectively. Ref. [11] Investigated the effect of MHD blood flow with velocity, thermal and concentration slip boundary layer with time dependent magnetic field. The study revealed that as the various parameter increases, the velocity, temperature and concentration of the blood increases. Refs. [11, 12] Investigated unsteady MHD blood flow with thermal radiation and chemical reactions under time-dependent magnetic field intensity. Results show that velocity increases with permeability and unsteadiness parameters, temperature increases with Prandtl and Hartmann numbers, and concentration decreases with Schmidt number. However, the model has shortcomings, including assuming uniform heat generation, neglecting buoyancy force and at the solution stage, the researcher abandoned the real system and pursuit the ghost of it.

Existing studies on the subject matter has largely failed to investigate the effects of heat and mass transfer of fluids with space dependent magnetic field, space dependent velocity, porosity effect of the media and non-uniform heat generation. From the literature, the studies on MHD fluids flow over the years have been by the use time dependent magnetic field and since it works very well. In recent time however, the cardiac issues from people need a severed thought from the physical point of view. The theoretical analysis used in the literature may not truly account for the cardiac problems that is alarming in the society. The application of external space dependent magnetic field, stretching velocity, permeability and non-uniform heat generation to model the effects of heat and mass transfer of fluids by fully retaining the intricacy of the fluids (blood) and media is to the best of our knowledge neglected in the literature. This work aims at distorting current models, to address the consequences of heat and mass transport in a nonlinear permeable medium.

2. Materials and methods

2.1. Theoretical consideration

The unsteady MHD flow model equations are formulated using the following assumptions:

i. A fluid is Newtonian, incompressible, radiates heat, reacts chemically, and conducts electricity.
ii. Blood is assumed to be MHD fluid here.
iii. The flow is characterized as laminar and erratic, with a two-dimensional (2D) plane in the media.
iv. The media is fixed, two-dimensional, porous and permeable on the surface and may be subjected to fluid suction or injection.
v. The magnetic field is space-dependent and acts in the same direction as the fluid flow.
vi. The flow media moves with velocity along the abscissa at time.

The study investigates two-dimensional unsteady MHD, incompressible laminar flow in a nonlinear permeable media with an external space-dependent magnetic field B(x) and a non-uniform heat source. The Lorentz force resists the flow in the presence of the applied magnetic field. The coordinate system measures the x-axis along the stretching media, the y-axis orthogonal to it and the fluid flow is occupied above the media for $y > 0$.

The external magnetic field $B(x)$ may be modelled using the relationship below:

$$B(x) = B_o \left(\frac{x}{\Omega}\right)^n. \tag{1}$$

Here, B_o is the magnetic field induction, x the distance along the media, Ω is the length of the media and n is a nonlinear stretching power of the media. The flow is influenced by the media wall's stretching motion, which can be modelled as follows:

$$U_s = U_o \left(\frac{x}{\Omega}\right)^n, \tag{2}$$

where U_o is the undisturbed velocity, x the distance along the media, Ω is the length of the media and n is a nonlinear stretching power of the media. The model depicts a magneto-hydrodynamic fluid stretched by a force in the flow direction, with surface temperature T_s and concentration C_s fluctuating with distance from the media slit at time t.

$$T_s(x) = T_\infty + D_1 \left(\frac{x}{\Omega}\right)^n, \tag{3}$$

$$C_s(x) = C_\infty + D_2 \left(\frac{x}{\Omega}\right)^n, \tag{4}$$

where T_∞ is the temperature of the fluid far away from the surface of the media, C_∞ *is the* concentration of the fluids far away from the surface of the media, x the distance along the media, Ω is the characteristics length of the media, n is a nonlinear stretching power of the media, and D_1 and D_2 are positive constants.

2.2. MHD flow equations models

Mathematical modeling of fluid flow use partial differential equations to reflect physics conservation laws, which regulate physical behavior under specified forces. Such as conservation of mass, Newton's second law of motion, and the first law of thermodynamics.

2.3. Mass continuity equation model

$$\frac{\partial u}{\partial x} + \frac{\partial v}{\partial y} = 0, \tag{5}$$

where u, v are velocity components and $x,\ y$ are coordinates.

2.4. Momentum equation model

The momentum equation model, based on Newton's second law, states that the rate change of a fluid's momentum is proportional to the external force exerted on it, influenced by various forces like gravity, viscosity, pressure, and electrostatics.

$$\frac{\partial u}{\partial t} + u\frac{\partial u}{\partial x} + v\frac{\partial u}{\partial y} = \eta\frac{\partial^2 u}{\partial y^2} - \frac{\sigma B^2(t)}{\rho}u - \frac{\eta}{\gamma_1\ (t)}u + g\beta_T (T - T_\infty) + g\beta_c (C - C_\infty), \tag{6}$$

Here, η is the viscosity of the fluid, and γ_1 is the permeability of the media, g is the acceleration due to gravity, β_T is the thermal expansion, β_c and is the thermometric concentration expansion. The space dependent permeability of the media γ_1 is assumed to be of the form:

$$\gamma_1\ (t) = \gamma_2 \left(\frac{x}{\Omega}\right)^n, \tag{7}$$

where γ_2 is the constant of permeability of the media, x the distance along the media, Ω is the characteristics length of the media and n is a nonlinear stretching power of the media. The nonlinearity of the media is retained because of the non-uniformity of the permeability parameter.

2.5. Energy equation model

The thermal energy equation model, based on the first law of thermodynamics, explains the rate of thermal energy change per unit volume.

$$\frac{\partial T}{\partial t}+u\frac{\partial T}{\partial x}+v\frac{\partial T}{\partial y}=\alpha\frac{\partial^2 T}{\partial y^2}+\frac{1}{\rho c_p}\Delta_h-\frac{1}{\rho c_p}\frac{\partial}{\partial y}\left(q_r\right). \tag{8}$$

Here, k is the thermal conductivity, c_p is the specific heat capacity of the fluid, $\Delta_h = q'''$ Heat generation/absorption in the Sinha's models, q_r is the radiative heat flux, ρ is the density of the fluid and α is the thermal diffusivity of the fluid.

The non-uniform heat generated or absorbed per unit volume in the media is calculated using the model below:

$$\Delta_h=\frac{kU_o}{x\eta}\left[A^*\left(T_s-T_\infty\right)e^{-\zeta}+B^*\left(T-T_s\right)\right], \tag{9}$$

where U_o is the free stream velocity, ζ is the similarity parameter A^* and B^* are non-dimensional parameters of space-dependent and temperature-dependent heat generation/absorption [13]. The radiative heat flux q_r, commonly known as the Rossland approximation, can be modeled as:

$$q_r=\left(-\frac{4\sigma^*}{3k^*}\right)\left(\frac{\partial T^4}{\partial y}\right). \tag{10}$$

Assuming that the differences in temperature within the flow are such that T^4 can be expressed as a linear combination of the temperature, we expand T^4 in Taylor's series about T_∞ as follow [13]:

$$T^4 = {T_\infty}^4+4{T_\infty}^3\left(T-T_\infty\right)+6{T_\infty}^2\left(T-T_\infty\right)^2+\ldots. \tag{11}$$

Linearizing the above equation, we have

$$T^4 \cong 4{T_\infty}^3T-3{T_\infty}^4, \tag{12}$$

Injecting equation (12) into equation (10), we have:

$$q_r=-\frac{16\sigma^*{T_\infty}^3}{3k^*}\frac{\partial T}{\partial y}. \tag{13}$$

After the replacement of the heat flux q_r, and heat generation parameter Δ_h, the energy equation (8) becomes:

$$\frac{\partial T}{\partial t}+u\frac{\partial T}{\partial x}+v\frac{\partial T}{\partial y}=\alpha\frac{\partial^2 T}{\partial y^2}+\frac{\alpha U_o}{x\eta}\left[A^*\left(T_s-T_\infty\right)e^{\zeta}+B^*\left(T-T_s\right)\right]+\frac{1}{\rho c_p}\frac{16\sigma^*{T_\infty}^3}{3k^*}\frac{\partial^2 T}{\partial y^2}, \tag{14}$$

2.6. Concentration equation model

The concentration of certain chemical components in fluids occurs at the body surface due to thermal equilibrium conditions, forming the concentration equation model of flow [11].

$$\frac{\partial C}{\partial t}+u\frac{\partial C}{\partial x}+v\frac{\partial C}{\partial y}=D_m\frac{\partial^2 C}{\partial y^2}-\delta\left(C-C_\infty\right). \tag{15}$$

Here, D_m is the mass diffusivity of the fluid, and δ is the reaction rate of the fluid.

2.7. The boundary conditions

The boundary conditions to the model equations for the simulation are:

$$\left.\begin{array}{l} u\left(x,0\right)=U_s,\ v=0,\ T\left(x,0\right)=T_s,\ \ C\left(x,0\right)=C_s \\ u\left(x,\infty\right)=0, v=0, T\left(x,\infty\right)=\ T_\infty,\ \ C\left(x,\infty\right)=C_\infty \end{array}\right\} \tag{16}$$

2.8. The stream function

In order to remove the continuity equation, a stream function ψ is introduced that satisfies the following relation:

$$\psi\left(x,y,t\right)=\int_0^y u dy, \tag{17}$$

such that

$$\begin{aligned} u\left(x,y,t\right)&=\frac{\partial\psi}{\partial y}, \\ v\left(x,y,t\right)&=-\frac{\partial\psi}{\partial x}. \end{aligned} \tag{18}$$

2.9. Non dimensionalization of the model equations

To represent several transport mechanisms in fluid dynamics, it is useful to state the conservation equations in non-dimensional form. The flow equations represent a system of coupled PDEs that are difficult to solve analytically. Similarity transformations are frequently used to convert such PDEs to a set of ODEs. The transformation to ODE was performed using the following non-dimensional variables:

$$\left.\begin{array}{c} x = \frac{\eta}{U_o} x^* \\ y = \frac{\eta}{U_o} y^* \\ t = \frac{1}{c} t^* \\ \zeta(x,y,t) = c\frac{y}{x} t \\ f(\zeta) = \frac{\psi(x,y,t)}{\sqrt{U_o \eta x}} \\ \theta(\zeta) = \frac{T - T_s}{T_\infty - T_s} \\ \Phi(\zeta) = \frac{C - C_s}{C_\infty - C_s} \end{array}\right\}. \tag{19}$$

Here, x^*, y^*denotes dimensionless coordinates, t^* non-dimensional time, c is the unsteadiness of the flow, ψ is dimensional stream function, ζ is the non-dimensional distance normal to the media of the flow, f is the non-dimensional stream function, c is the unsteadiness parameter, θ is the non-dimensional temperature of the fluid and Φ is the non-dimensional concentration of the fluid.

2.10. Transformation of the model equations for simulation

The approach of similarity transformations with non-dimensional variables equation (19) yields the local solution to the momentum model, heat equation model and concentrations equation model (6), (8) and (15), in non-dimensional ODEs (20), (21) and (22), respectively.

$$\chi f''' - \left(\tau\zeta - \frac{1}{2}f - \frac{\zeta}{2}f\right) f'' - \left(\tau - M^2 - \gamma_3\right) f' + \frac{1}{2} f'^2 + \gamma_t\theta + \gamma_m\Phi = 0, \tag{20}$$

$$q\left(\frac{1}{\mathrm{Pr}} + R\right)\theta'' + \left(p + \frac{1}{2}f\right)\theta' - \frac{l}{\mathrm{Pr}}\left[A^* e^{-\zeta} + B^*\theta\right] - nf'\,\theta + nf' = 0, \tag{21}$$

$$\frac{q}{Sc}\Phi'' + \left(p + \frac{1}{2}f\right)\Phi' + \delta^*\Phi - nf'\Phi + nf' = 0, \tag{22}$$

where $\tau = \frac{\eta c x^{*2}}{U_o{}^2 t^*}\sqrt{\frac{1}{x^*}}$ be unsteadiness parameter, $\chi = t^*\sqrt{\frac{1}{x^*}}$, $M^2 = \frac{B_o{}^2\eta^3 x^{*\left(\frac{3+2n^2}{2}\right)}\sigma}{U_o{}^4\Omega^{n^2} t^*\rho}$ be magnetic field parameter, $\gamma_3 = \frac{\eta\Omega^n x^{*\left(\frac{3-2n}{2}\right)}}{\gamma_2 U_o t^*}$ be permeability parameter, $\gamma_t = \frac{\eta x^{*2} g\beta_T}{U_o{}^3 t^{*2}}(T_\infty - T_s)$ be thermal Grashof number and $\gamma_m = \frac{\eta x^{*2} g\beta_c}{U_o{}^3 t^{*2}}(C_\infty - C_s)$ be concentration Grashof number, $p = \frac{\eta c y^*\sqrt{x^*}}{U_o{}^2 t^*}$, $l = \frac{\sqrt{x^*}}{t^*}$, $q = \frac{t^*}{\sqrt{x}}$, $Pr = \frac{\eta}{\alpha}$ be Prandtl number and $R = \frac{1}{\rho c_p}\frac{16\sigma^* T_\infty{}^3}{3k^*\eta}$ be radiation parameter, $Sc = \frac{\eta}{D_m}$ Schimidt number, $q = \frac{t^*}{\sqrt{x}}$ constant and $\delta^* = \frac{\eta\delta x^*\sqrt{x^*}}{t^* U_o{}^2}$ chemical reaction parameter.

2.11. The boundary conditions of the non-dimensional models

The boundary conditions corresponding to the simulations equations (20), (21) and (22) are given by:

$$\left.\begin{array}{l} f(0) = f_w,\ f'(0) = 1,\ \theta(0) = 0\ and\ \ \Phi(0) = 0 \\ f'(\zeta) \to 0,\ \ \theta'(\zeta) \to 0\,,\ \Phi'(\zeta) \to 0\ as\ \zeta \to \infty \end{array}\right\}. \tag{23}$$

Here, f_w denote suction and injection parameters, respectively. If $f_w > 0$ connotes suction and $f_w < 0$ connotes injection.

2.12. Skin-friction, local Nusselt number and Sherwood number

The skin- friction coefficient C_{f_x}, the rate of heat transfer coefficient (local Nusselt number Nu_x) and the rate of mass transfer coefficient (Sherwood Number Sh_x) are the important parameters in thermal Engineering and Physics applications. They can be obtained from the following relations [14]. The Skin-friction coefficient $C_{\mathrm{fx}}$is defined as:

$$C_{\mathrm{fx}} = \frac{\tau_w}{\rho U_w{}^2}, \tag{24}$$

where τ_w is the local shear stress which is defined as:

$$\tau_w = -\mu\left(\frac{\partial u}{\partial y}\right)_{y=0}. \tag{25}$$

Table 1: Fluid properties.

Parameter	Value	Unit
Viscosity of Blood, μ	3.20×10^{-3}	$\mathrm{kg}m^{-1}s^{-1}$
Density of Blood, ρ	1.06×10^{3}	$\mathrm{kg}m^{-3}$
Specific heat capacity of blood, c_p,	3.90×10^{3}	$J\mathrm{kg}^{-1}K^{-1}$
Electrical conductivity Blood, σ	5.0×10^{-1}	$S\,m^{-1}$
Thermal conductivity of the fluid, k	1.20×10^{-7}	$Wm^{-1}K^{-1}$

The rate of heat transfer coefficient or Nusselt number Nu_x is defined as:

$$\mathrm{Nu}_x = \frac{q_w x}{k\,(T_w - T_\infty)}, \tag{26}$$

where q_w is the heat flux or the local heat transfer rate given as:

$$q_w = -k\left(\frac{\partial T}{\partial y}\right)_{y=0}. \tag{27}$$

The rate of mass transfer coefficient or Sherwood number Sh_x is defined as:

$$\mathrm{Sh}_x = \frac{m_w x}{D_m\,(C_w - C_\infty)}, \tag{28}$$

where m_w is the mass flux or mass transfer rate respectively. It is given as:

$$m_w = -D_m\left(\frac{\partial C}{\partial y}\right)_{y=0}. \tag{29}$$

2.13. Transformation of the skin-friction coefficient $\mathbf{C}_{fx}$ Nusselt number $Nu_{\mathbf{x}}$ coefficient and Sherwood number $Sh_{\mathbf{x}}$ Coefficient

The approach of similarity transformations with non-dimensional variables equation (19) yields the local solution to the $\mathrm{C_{fx}}$, $\mathrm{Nu_x}$ and $\mathrm{Sh_x}$ equations (24), (26), and (28), in non-dimensional ODE (30), (31), and (32), respectively.

$$t^{*-2}x*^{\frac{3}{2}}\,C_{fx} = -f'', \tag{30}$$

$$t^{*-1}\mathrm{Nu}_x = -\theta', \tag{31}$$

$$t^{*-1}Sh_x = \Phi'. \tag{32}$$

In order to obtain the solutions numerically, it is pivotal to give the parameters in the problem under investigation some numerical values. Here, we considered human blood at 37^oC.

2.14. Simulation methods

The study employs the Runge-Kutta Fehlberg and Newton-Raphson methods, selected for their ability to solve nonlinear differential equations with both precision and efficiency. The Runge-Kutta Fehlberg method provides adaptive step-sizing that optimizes accuracy while minimizing computational time, a critical consideration for modeling nonlinear MHD flows where dynamic changes in fluid properties occur. The Newton-Raphson method enhances convergence, especially when dealing with highly nonlinear systems. While alternative methods, such as finite element and finite difference methods, are often used in similar studies, these methods were chosen for balancing computational feasibility and accuracy. Additionally, potential limitations, such as step size sensitivity in the Runge-Kutta Fehlberg method, were carefully managed to ensure stability in results. Tables 1-4 show the physiological results for human blood at a temperature T of $310k$ based on the experimental studies of Ref. [15].

2.15. Computational flowchart

The following computational flowchart illustrates the systematic approach undertaken in this study to analyze unsteady magnetohydrodynamic (MHD) fluid flow within a nonlinear permeable medium. It outlines the key steps involved in, implementing numerical methods, and examining the thermochemical effects related to heat and mass transfer. This visual representation serves as a roadmap for the research process, ensuring clarity and coherence in the execution of the computational tasks necessary for achieving the study's objectives.

Table 2: Simulation parameters.

Parameter	Value	Unit
Length of the media, Ω	1.000	m
Unsteadiness constant, c	0.833,4.1667, 12.50, 16.6667	s^{-1}
Undisturbed velocity, U_o	0.005	ms^{-1}
Rate of mass transfer, δ	100.0	s^{-1}
Magnetic field,B_o	0.0, 256.0, 296.6, 330	T
Reference permeability,$\gamma_1 \times 10^{-5}$	5.0, 6.0, 7.5, 12.0	m^2
Roseland coefficients, $k^* \times 10^{-2}$	7.989875184, 2.663291728, 1.597975037, 0.7989875184	m^{-1}
Thermal expansion coefficient, β_T	0.00043, 0.00088, 0.0016, 0.00213	K^{-1}
Concentration l expansion coefficient,	4.30, 6.40, 8.51, 10.63	$\mathrm{dm^3 mol^{-1}}$
Mass diffusivity $D_m \times 10^{-5}$,	30.0, 6.0, 3.0, 0.1875	$m^2 s^{-1}$
Stefan's Boltman constant, σ^*	5.67×10^{-8}	$Wm^{-2}K^{-4}$
Surfaces temperature, T_s	310.0	K
Ambient temperature, T_∞	320.0	K
Surface concentration, C_s	0.01	$\mathrm{moldm^{-3} moldm^{-3}}$
Surface concentration, C_∞	0.02	$\mathrm{moldm^{-3} moldm^{-3}}$
Non-dimensional time, t^*	1.000	-
Non-dimensional y-coordinates , y^*	1.000	-
Non-dimensional x-coordinates , x^*	1.000	-

Table 3: Computed parameters.

Parameter	Value
Magnetic parameter, M	0.0, 1.5, 2.0, 2.5
Unsteadiness constant, τ	0.1, 0.5, 1.5, 2.0
Permeability parameter, γ_3	5.0, 8.0, 10.0, 12.0
Thermal Grassoff Number, γ_t	1.0, 2.1, 3.8, 5.0
Concentration Grassoff Number, γ_m	1.0, 1.5, 2.0, 2.5
Prandtl Number, Pr	0.72, 10, 20, 25
Schimidt Number, Sc	0.01, 0.05, 1.0, 1.6
Radiation parameter, R	10.0, 30.0, 50.0, 100.0
Rate of mass transfer, δ	0.05, 5.0, 10.0, 12.0
$p,\ q$	1.0000000000
l	1.0000000000

Table 4: Boundary values.

Parameter	Value
Wall porosity, fw	1.0, -0.1, -0.5, 3.0
Space dependent heat generation parameter, A^*	0, -30, 5, 10
Temperature dependent heat generation parameter, B^*	0.0, -50.0, 5.0, 15.0

3. Results

The physics that took place in the flow regime in the media is revealed in the present part for the computations of the velocity field $f(\zeta)$, temperature field $\theta(\zeta)$ and the mass concentration field $\Phi(\zeta)$ for various values of the flow parameters, which define the flow features. Additionally, the skin friction coefficient C_{fx}, Sherwood number Nu_x, and Nusselt number Sh_x are computed. The following flow parameters are used to graph all of the results: M magnetic parameter, γ_3 permeability parameter, γ_t thermal Grashof number, γ_m concentration Grashof number, Pr Prandtl number, Sc Schimidt number,R radiation parameter, δ^* chemical reaction, parameter f_w wall porosity of the wall, A^*space dependent heat generation parameter, B^* temperature dependent heat generation parameter and τ unsteadiness parameter.

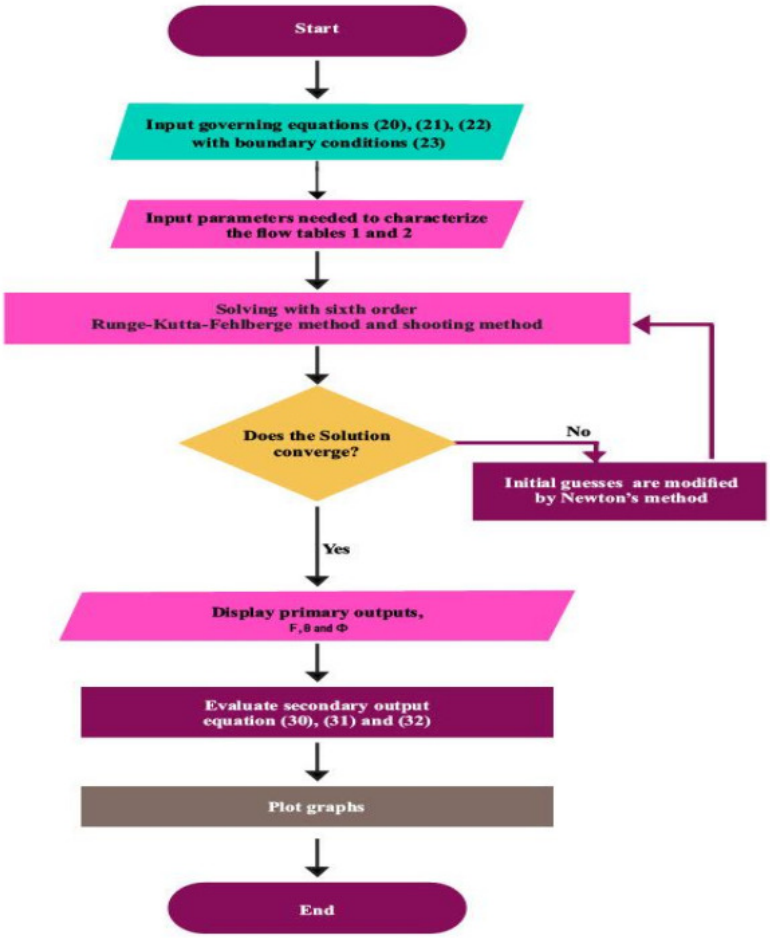


Figure 1: Computational flowchart.

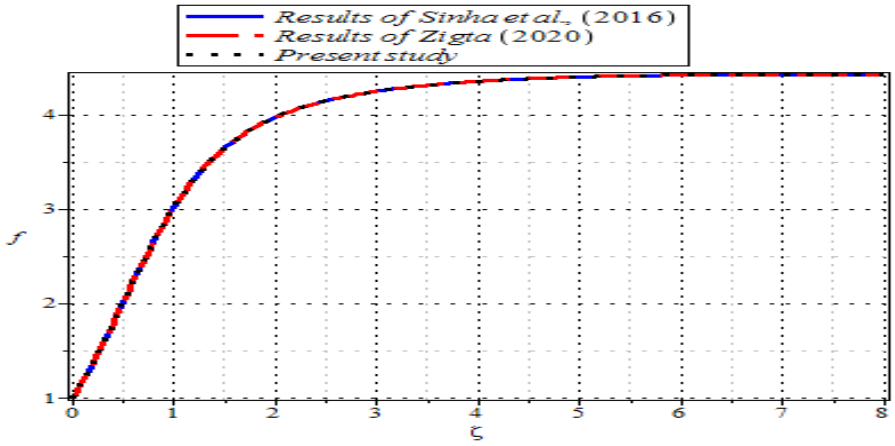


Figure 2: Velocity profile for comparison of presents results and literature works.

3.1. *Temperatures profiles*

The effects of parameter modifications on temperature distribution are presented in Figures 12-18.

3.2. *Concentration profiles*

The effects of parameter fluctuations on concentrations are shown in Figures 19-27.

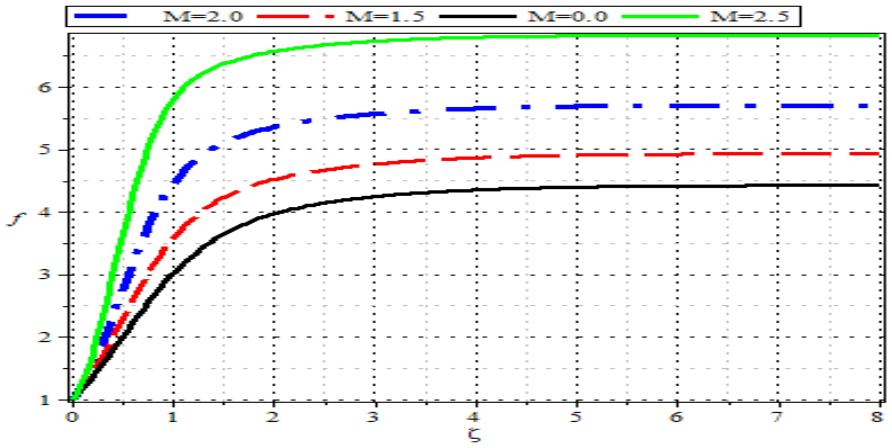


Figure 3: Velocity profile for different values of Magnetic parameter.

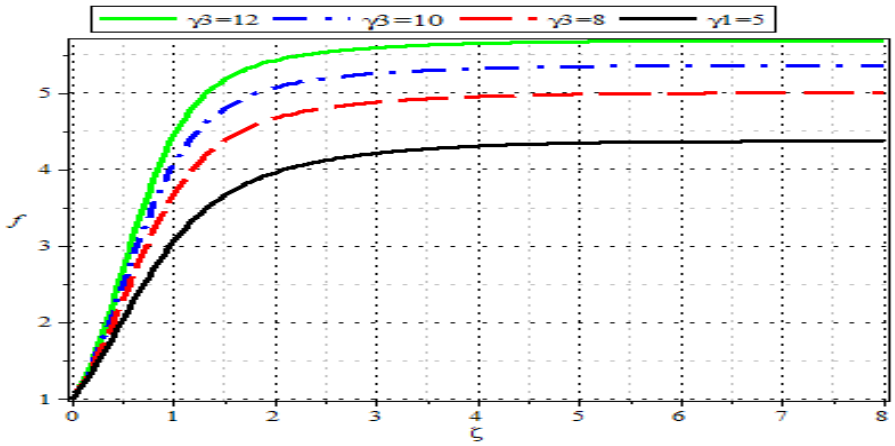


Figure 4: Velocity profile for different values of permeability parameter.

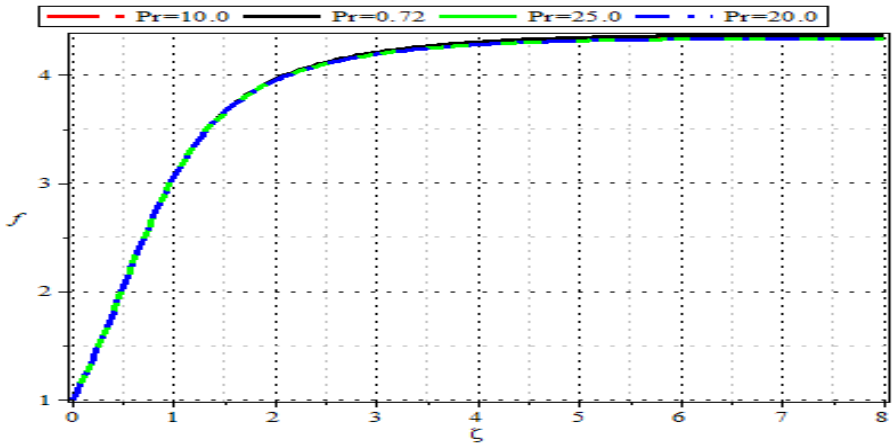


Figure 5: Velocity profile for different values of Prandtl number

3.3. Discussion of results

3.3.1. Velocity profiles

It is observed that, at the surface of the media, the fluid velocity is typically zero. It then grows to the specified undisturbed region of the flow (free stream value), satisfying the far field boundary condition. Figure 2 shows the velocity profiles with comparison to Refs. [7, 8]. It is noticed from Figures 2-4 and 6-8 that, as the magnetic parameter M, permeability parameter γ_3, Prandtl number Pr,

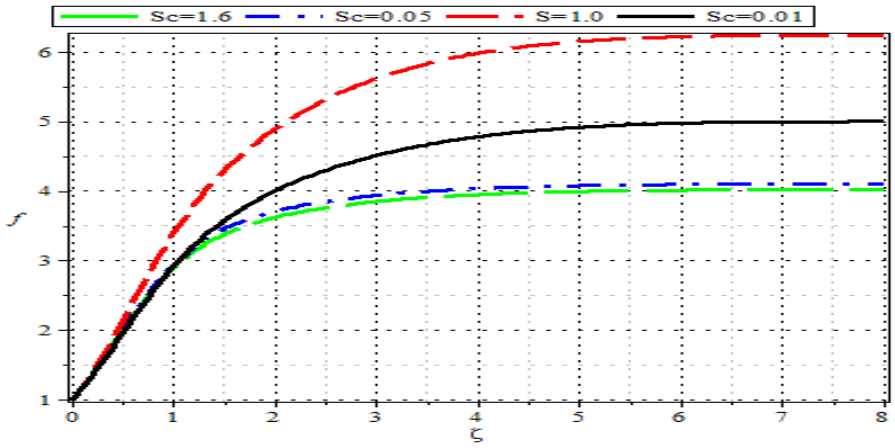


Figure 6: Velocity profile for different values of Schimidt number.

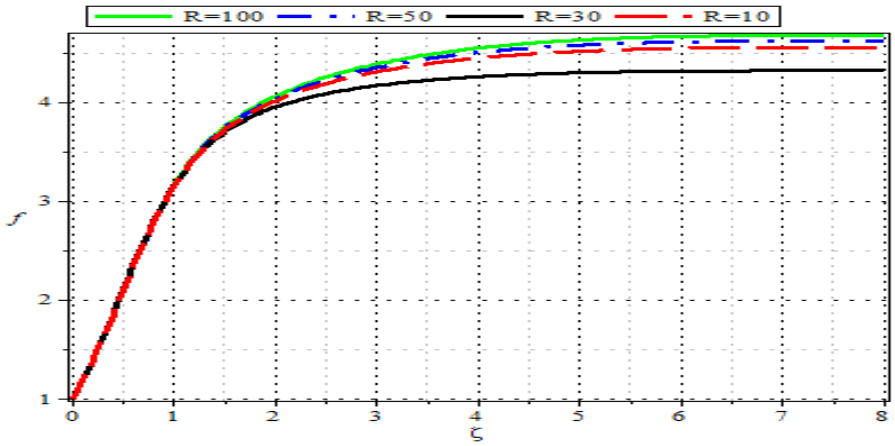


Figure 7: Velocity profile for different values of radiation parameter.

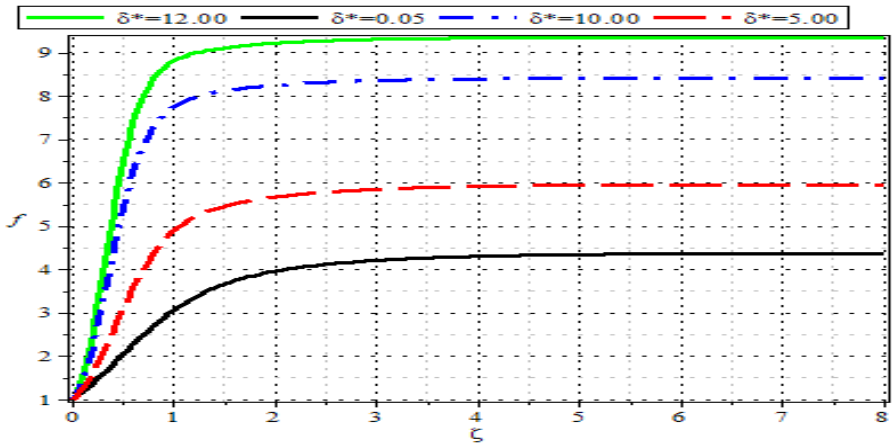


Figure 8: Velocity profile for different mass transfer parameter.

radiation parameter R, mass transfer δ^* parameter and wall porosity parameter fw increase, and the velocity profiles also increase. All of these profiles increased rapidly and tend asymptotically to the unperturbed region of flow away from the media. The increment of the profiles observed in Figures 2–4 and 8 leads to an increase in fluid mobility in the media surface. It also suggests that the electromagnetic Lorentz force pushes the electrically conducting fluid in the direction of the permeable media surface. This explains why an electrically conducting fluid in the micro scale system may be advanced by the magnetic field. It is also important to note that

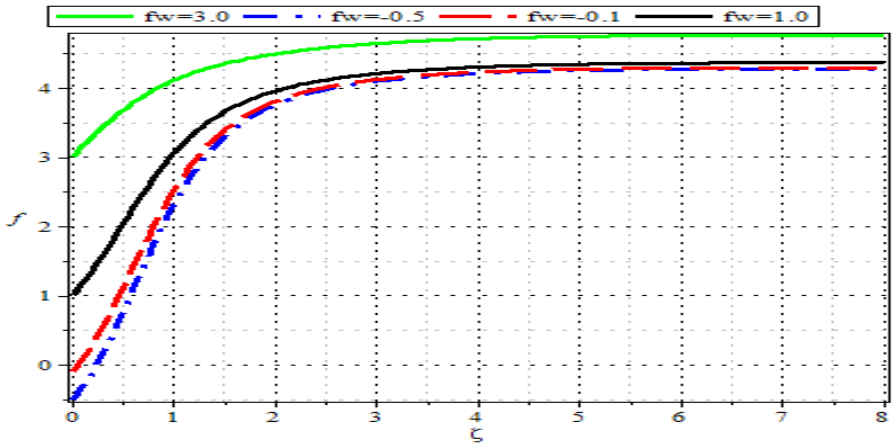


Figure 9: Velocity profile for different values of wall porosity parameter.

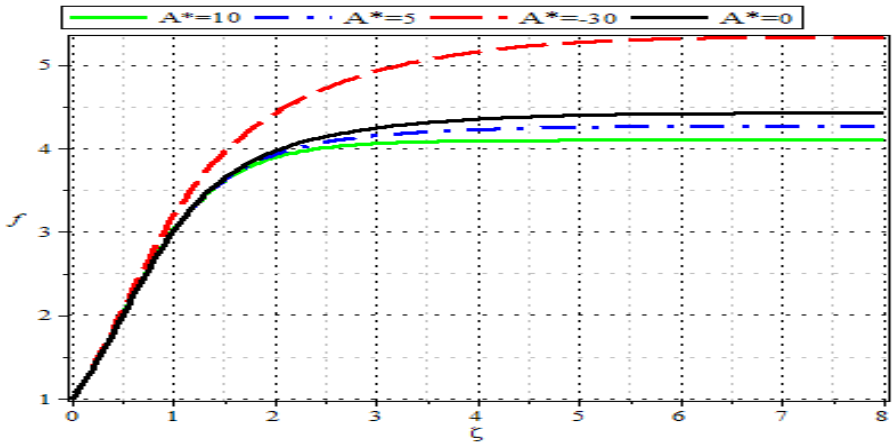


Figure 10: Velocity profile for different values of space dependent heat generation parameter.

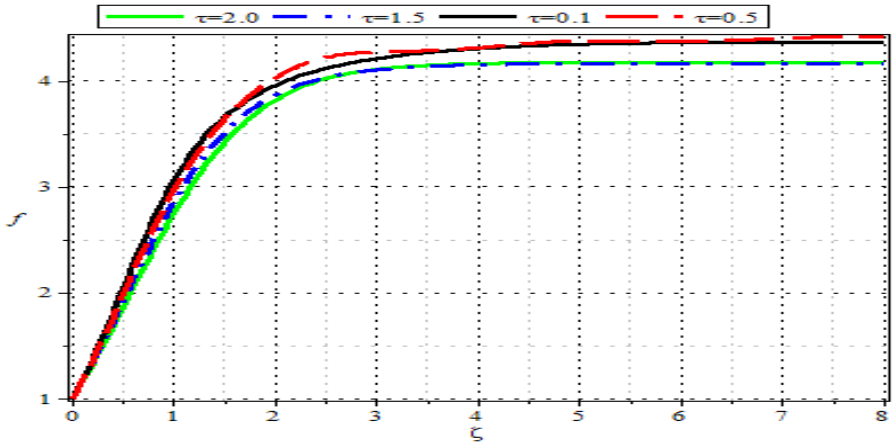


Figure 11: Velocity profile for different values of unsteadiness parameter.

the fluid is pushed in the same direction toward the media surface by buoyant force brought on by temperature differences, radiation absorption, and fluid suction as noticed from Figures 2–4 and 8. We can see in Figures 5-10 that the velocity profiles decrease when the Schimidt number Sc, space dependent and temperature dependent heat generation parameters A^*, B^* and unsteadiness parameter τ increase. The decrease of the profiles could be explained by the combined effects of a drop in fluid thermal diffusivity and more hot fluid being injected into the flow regime. The non-sensitivity of Prandtl Number to velocity profiles observed in Figure 4 may

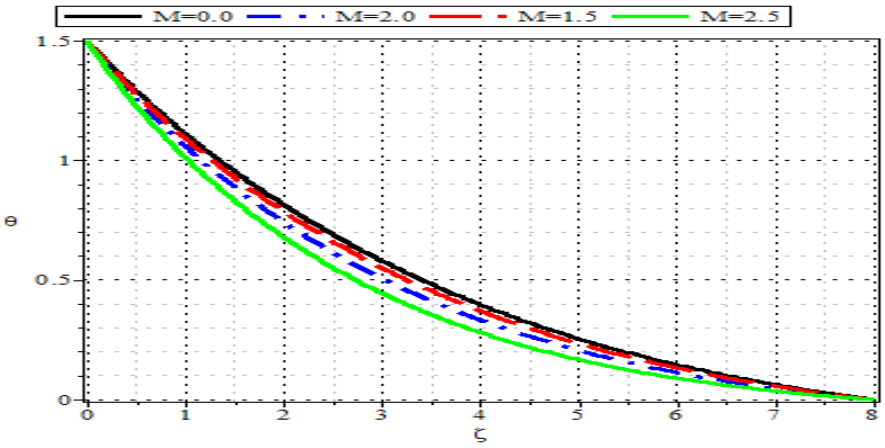


Figure 12: Temperatures profiles for different values of Magnetic parameter.

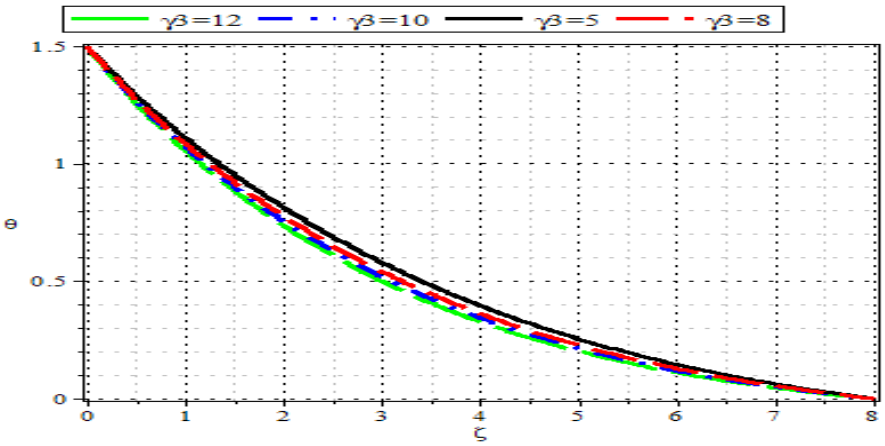


Figure 13: Temperatures profiles for different values of permeability parameter.

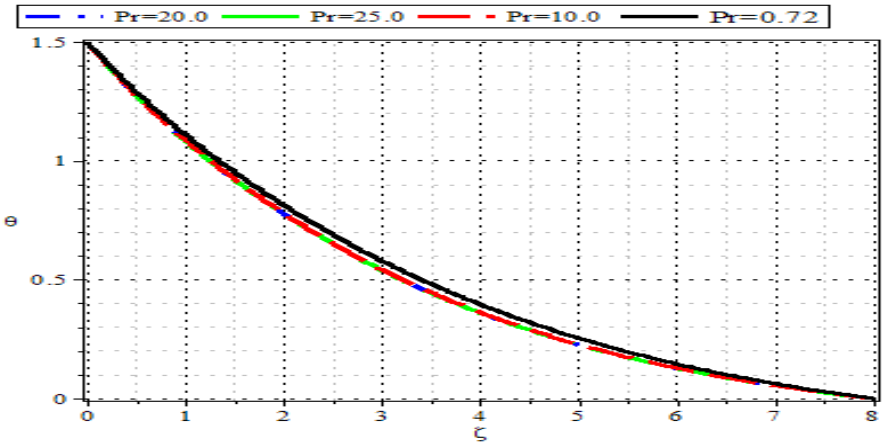


Figure 14: Temperatures profiles for different values of Prandtl number.

be attributed to dominant momentum diffusion, decoupling of momentum and thermal transport and non-linear interactions between momentum, heat, and mass transport. When the momentum diffusion is much faster than thermal diffusion, the Prandtl number becomes less sensitive and non-linear interactions between momentum, heat, and mass transport can reduce the sensitivity of profiles to the Prandtl number.

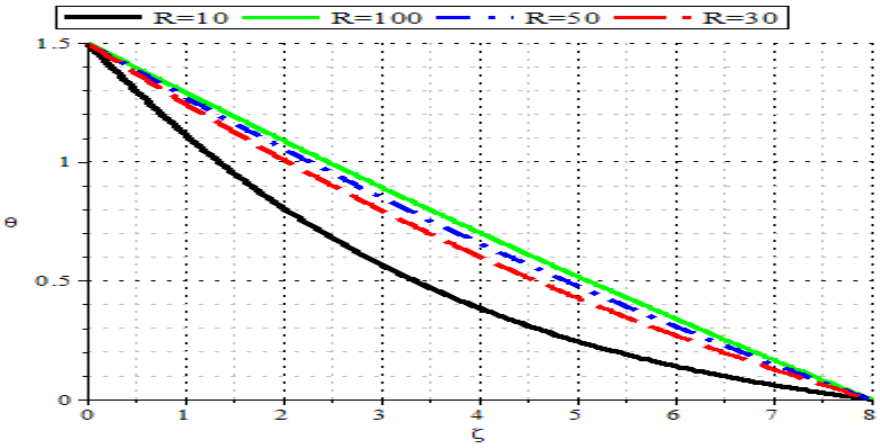


Figure 15: Temperatures profiles for different values of radiation parameter.

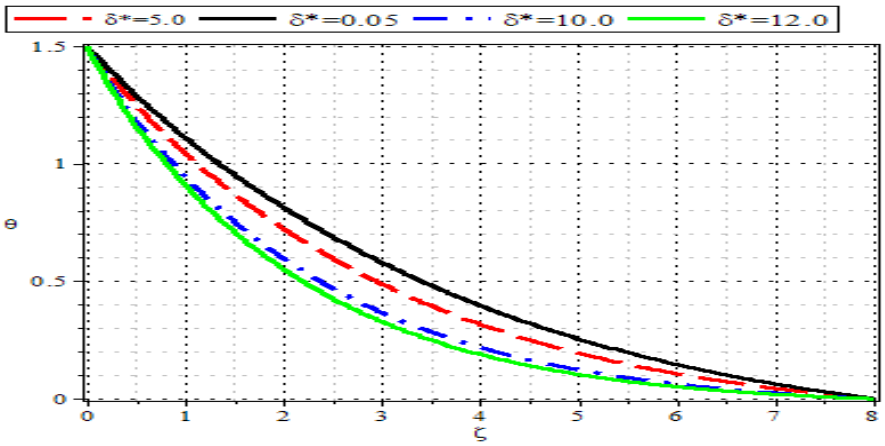


Figure 16: Temperatures profiles for different values of mass transfer parameter.

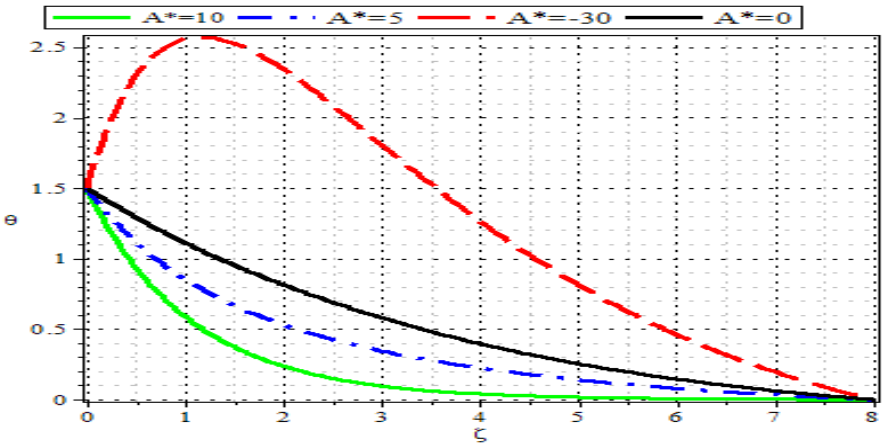


Figure 17: Temperatures profiles for different values of space dependent heat generation parameter.

3.3.2. *Temperatures profiles*

Similar trend of a decline in the fluid temperature and temperature profiles is observed in Figures 16 and 17 when space dependent heat generation parameter $A^* \geq 0$ and temperature dependent heat generation parameters $B^* \geq 0$. The declined in the temperature profiles observed in Figures 12, 15-17 were due to Joule heating, also known as Lorentz heating because of the applied magnetic field and heat generated by fluid, which induce an extra heat source in the flow system which raises the fluid's temperature in the media.

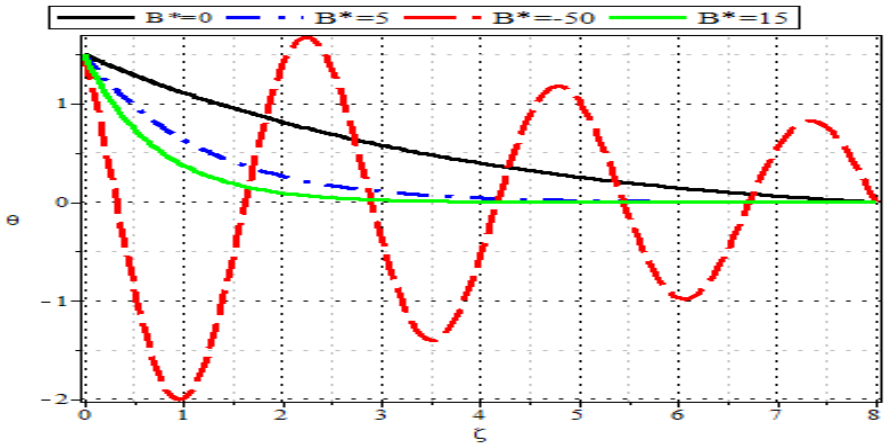


Figure 18: Temperatures profiles for different values of temperature dependent heat generation parameter.

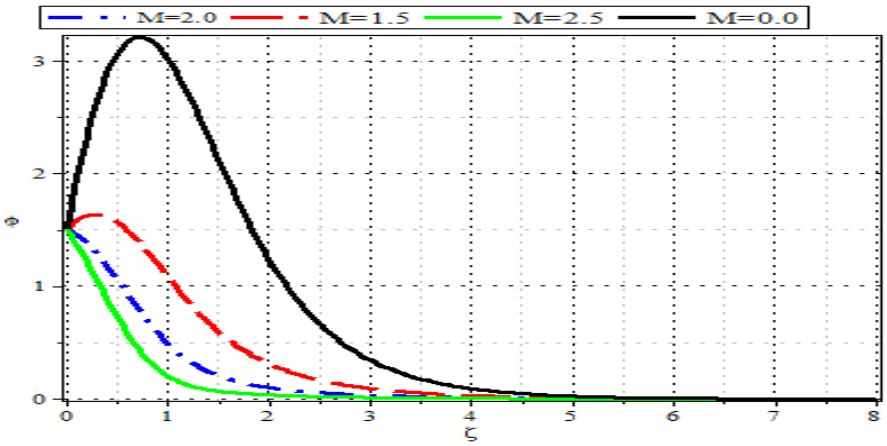


Figure 19: Concentration profiles for different values of Magnetic parameter.

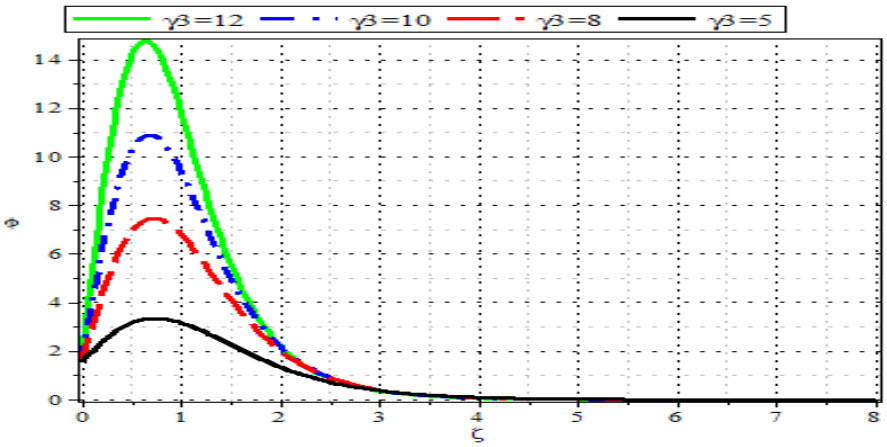


Figure 20: Concentration profiles for different values of permeability parameter.

A reverse trend is observed in Figures 14, 15–18. The fluid temperature and temperature profiles increase as radiation parameter R increase, space dependent heat generation $A^* < 0$ and temperature dependent heat generation parameters $B^* < 0$ respectively. This increase in fluid temperature observed in Figures 14, 17, and 18 may be attributed to the absorption of heat by the fluid from the media surface leading to surface cooling and the viscous.

The attenuated oscillations observed in Figures 17 and 18 may be attributed to many factors. Among them are; thickness and

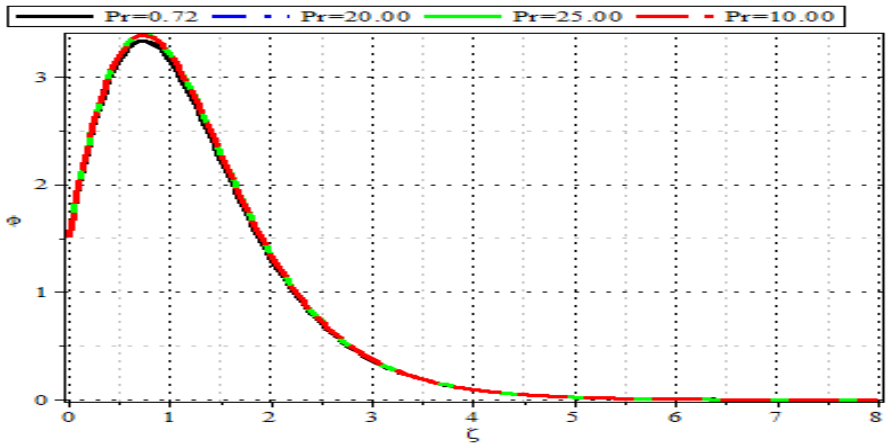


Figure 21: Concentration profiles for different values of Prandtl number.

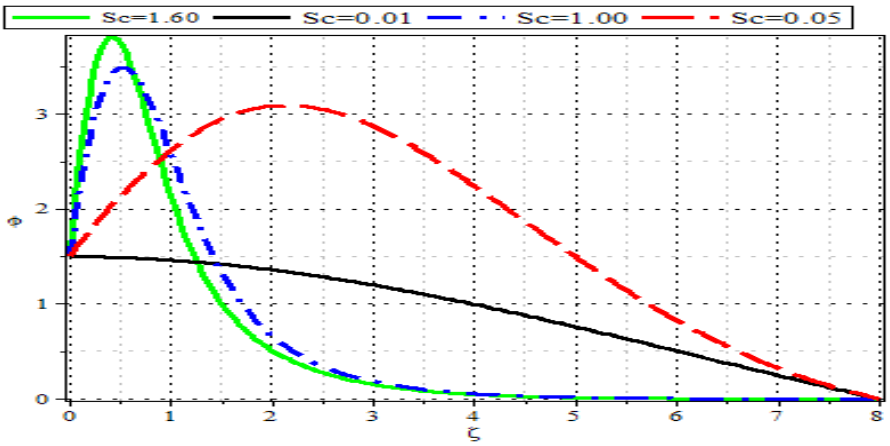


Figure 22: Concentration profiles for different values of Schimidt number.

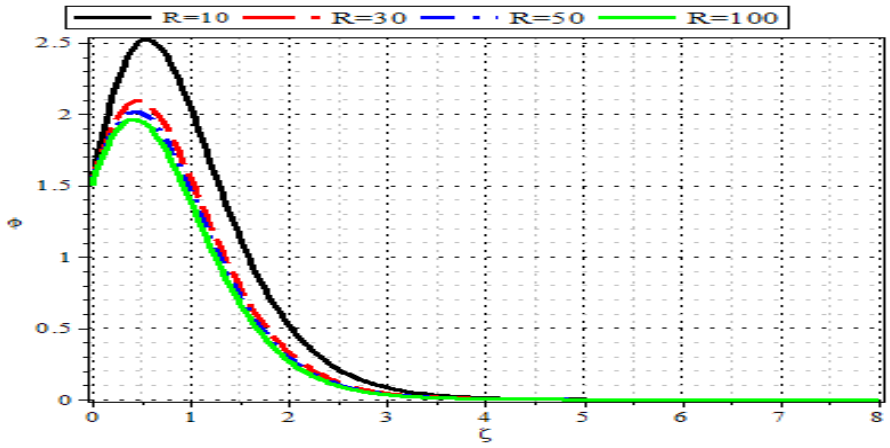


Figure 23: Concentration profiles for different values of radiation parameter.

resistance of the fluid, the ability of the media wall to stretch and expand, Turbulent flow. With the above, the flow oscillations may be attenuated thereby lowering the flow of the fluid which may lead to chaos. This results may have potential application in therapeutic procedure of electrometric hypothermic treatment of cancer where the blood viscosity requires control with respect to temperature variation.

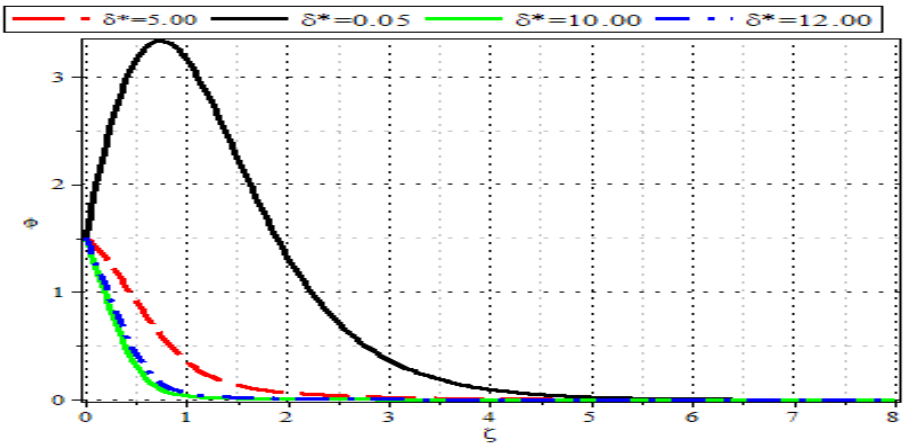


Figure 24: Concentration profiles for different values of mass tranfer parameter.

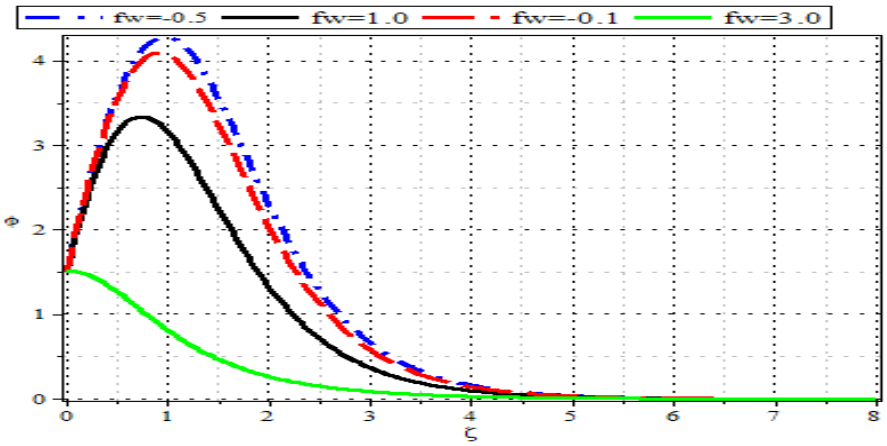


Figure 25: Concentration profiles for different values of wall porosity parameter.

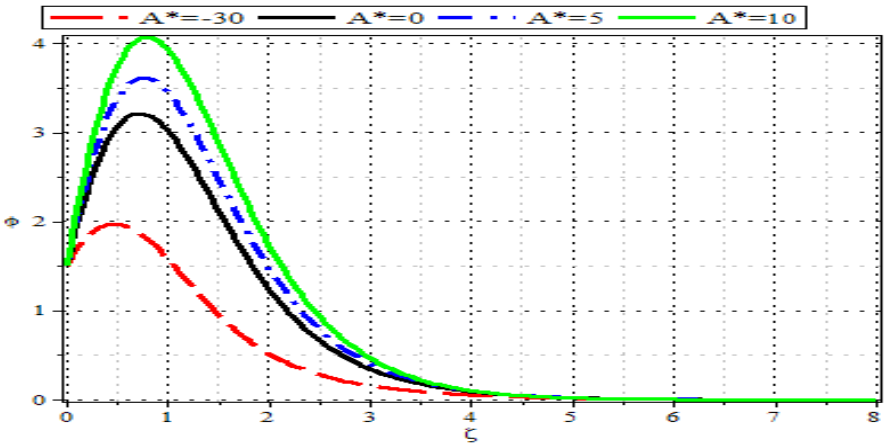


Figure 26: Concentration profiles for different values of space dependent heat generation parameter.

3.3.3. Concentration profiles

The effects of parameter fluctuations on concentrations are shown in Figures 19–27. We see that the concentration profile behaves differently before and after particular points of ζ. For $\zeta < 0.5$, the concentration distribution increase, then declines exponentially when $\zeta > 0.5$. We noticed two distinct sorts of behavior in the concentration profile as magnetic parameter M, permeability parameter γ_3, Schimidt number Sc, δ^* mass transfer parameter, and wall porosity of the wall f_w increases along the domain shown

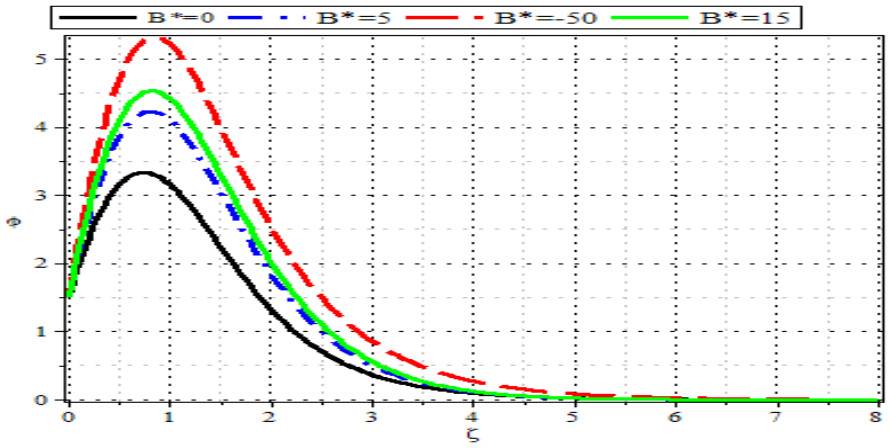


Figure 27: Concentration profiles for different values of temperature dependent heat generation parameter.

in Figures 19-24, that is, the concentration profiles increase and decline exponentially to the free stream region. It also increases when $\delta^* < 1$ as observed in Figure 24. The opposite trend is exhibited as those parameters get higher. These increase in the concentration profiles may be attributed to accumulating or building up species in the media potentially leading to saturation or maximum capacity. A decrease in the concentration profiles were observed in Figures 19 and 24 when $M \geq 2$ and $\delta^* > 1$. These decrease in concentration profiles observed may be attributed to the following; reduced concentration gradients within the fluid, faster mixing and homogenization of the fluid in the media and enhanced mass transfer rates, leading to faster dissolution, or absorption processes. In summary, a decreasing concentration profile indicates faster mixing, enhanced mass transfer, and reduced concentration gradients, leading to improved process efficiency, product quality, and scalability, as well as energy savings.

The findings of this research provide critical insights into the role of magnetohydrodynamic (MHD) principles in biomedical applications, particularly regarding their influence on blood flow within permeable vessels. The study demonstrates that the manipulation of MHD fluid dynamics can significantly impact blood circulation, offering potential advancements in targeted drug delivery systems. By leveraging external magnetic fields, it may be possible to guide magnetically tagged therapeutic agents to specific areas of the body, enhancing treatment precision while minimizing systemic exposure.

Moreover, the findings reveal the physiological implications of parameters such as magnetic field strength and thermal gradients. Variations in these factors can alter blood viscosity and flow rates, affecting the efficiency of nutrient and oxygen delivery to tissues. For instance, an increase in magnetic field intensity could enhance the alignment of red blood cells, potentially improving flow characteristics in narrow vessels, which is crucial during medical interventions. Similarly, the thermal gradients identified in the study can influence local tissue temperatures, thereby impacting metabolic processes and healing rates.

By establishing a concrete connection between the computational model and real-world biomedical applications, this research underscores the potential of MHD principles to innovate medical procedures. The insights gained from the model not only contribute to a better understanding of fluid dynamics in biological systems but also pave the way for the development of advanced medical technologies aimed at improving patient outcomes in various clinical scenarios.

3.4. Comparative analysis

In our investigation of magnetohydrodynamic (MHD) fluid flow in nonlinear permeable media, we have conducted a comparative analysis against existing literature that addresses similar MHD flow parameters such as studies by Zigta [11] and Sinha *et al.* [7]. Our findings demonstrate alignment with previous research, particularly illustrated in Figure 2, which confirms trends regarding the influence of magnetic fields on flow stability and uniformity. This corroboration highlights the consistency of our results with established theories in the field. However, we also identified significant deviations in the results presented in Figures 2 and other figures, which diverges from conventional MHD behavior observed in similar setups. These figures reveal unique velocity, temperature profiles and mass transfer characteristics that differ from those typically reported in the literature. The differences suggest that the interplay between thermal gradients and magnetic fields in our specific nonlinear permeable medium may introduce behaviors not accounted for in previous studies.

To elucidate these observed deviations, we propose that the distinct properties of the permeable medium significantly impact the interaction dynamics between the magnetic and thermal influences. In our model, the nonlinear characteristics of the medium appear to amplify certain effects, leading to altered fluid dynamics and temperature distributions. This insight prompts a reevaluation of conventional MHD frameworks when applied to permeable materials, as it underscores the complexity introduced by nonlinear interactions. By comparing our findings to established literature, we not only reinforce the validity of our results but also highlight areas where further research is warranted. This comparative analysis opens avenues for a deeper understanding of MHD phenomena

in biomedical contexts, such as optimizing blood flow in medical applications and enhancing the design of therapeutic delivery systems. Our unique findings pave the way for future studies aimed at unraveling the intricate relationships between MHD behavior and the physical properties of permeable media

4. Conclusion

The nonlinear mathematical models of the unsteady MHD flows of heat and mass through a permeable media were formulated and the thermal and mass transfer effects of unsteady MHD fluids flow in permeable media subjected to a combined action of a transverse magnetic field intensity and buoyancy force have been analyzed and discussed in the last section.

Using similarity variables, the model partial differential equations were transformed into a set of nonlinear coupled ordinary differential equations. A numerical algorithm were developed based on shooting technique coupled with Runge-Kutta Fehlberg integration technique.

The model equations were computationally studied using the numerical algorithm developed and the results were presented and discussed accordingly. Graphical results were presented for the fluid velocity, temperature and concentration profiles, local skin friction coefficient, local Nusselt and Sherwood number.

The study bears the potential to explore some important information regarding the complex flow behavior of fluids in situations where all the physical parameters M,γ_3, γ_t, γ_m, Pr, R, δ^*, fw, Sc, A^*, B^* and τ play prominent roles in the flow with heat and mass transfer in small blood vessels. The main findings can be summarized as follows:

i. By the application of sufficiently strong magnetic field M parameter, permeability parameter γ_3, thermal Grashof number γ_t, concentration Grashof number γ_m , Prandtl number Pr, radiation parameter R, mass transfer δ^* parameter and wall porosity parameter fw, fluid velocity increased. The fluids velocity can be diminished when Schimidt number Sc, space dependent heat generation parameter A^*, temperature dependent heat generation parameter B^* and unsteadiness parameter τ increase. The results presented may be of significant interest to surgeons who usually want to keep the blood flow rate at a desired level during the entire surgical procedure.

ii. With a rise in heat generation, the temperature of the fluid may increases, but a reverse trend were observed in the case of heat absorption. This observation may be of particular importance in the therapeutic procedure of electromagnetic hyperthermia used in the treatment of cancer, because the therapy involves rising the temperature of the cancerous tissues above 42^{o}C. An increase in temperature brings down fluid viscosity. While applying the procedure of hyperthermia, it is necessary to see that blood viscosity does not increase, because in that case there may arise various problems in respect of circulation of blood.

iii. The mass transfer, magnetic field parameters, and concentration Grassof Number has a dual effect on the concentration profiles. The concentration increases in the flow assisting region ($\delta^* < 1, M < 2$ *and* $\gamma_m < 1.7$) and decreases in the flow opposing region ($\delta^* > 1, M \geq 2$)2 *and* $\gamma_m > 1.7$.

iv. The skin friction coefficient, Nusselt and Sherwood Numbers increases for small values of the parameters M,γ_3,γ_t, γ_m, Pr, R, δ^*, fw, Sc, A^*, B^* and τ and diminishes for larger values of the parameters.

Finally, it is evident that the heat and mass transfer effects on unsteady MHD fluids flow through a permeable surface with thermal radiation can be enhanced using appropriate combination of thermo physical parameter values for efficient operation. The results may be applied to improve the design of a variety of flow and thermal systems including micro scale systems such as micro mixing technologies. It is hoped that the present work will serve as a stimulus for experimental work to clinicians, surgeons and biomedical engineers, because they serve as useful estimates, which are capable of throwing some light toward the understanding of fluids flow in biological systems.

4.1. Limitation of the findings

While this study provides valuable insights, it also operates within certain limitations. Assumptions such as uniform media properties and two-dimensional modeling simplify the system but may not fully capture complex interactions present in real biological or industrial environments. Additionally, factors like permeability variability and non-uniform thermal diffusivity in biological systems could influence flow characteristics, suggesting the need for three-dimensional models in future research. Furthermore, this model's theoretical nature underscores the need for experimental validation, particularly in biomedical contexts where biological variability can significantly impact flow behavior. Future studies should explore these aspects to develop more comprehensive models that can be applied to practical scenarios.

Data availability

In accordance with the university's policies, the data is available through the school. For further inquiries, interested individuals may contact the author via email at denensolomon41@gmail.com.

Acknowledgment

The authors are grateful to God for the good health and well-being that were necessary to complete this research work. D. S. Igba wishes to extend his sincere gratitude to Prof. I. M. Echi, who has the mind of an expert. He patiently instructed and encouraged me to think big and not to give up when all seemed not to be working out. Without his unique assistance, the goal of this research would never have been realized.

References

[1] A. Farhad, I. Anees, A. Khan, K. Ilyas, A. Irfan & Badruddin, "Effects of MHD and porosity on entropy generation in two incompressible Newtonian fluids over a thin needle in a parallel free stream", Scientific Reports **10** (2020) 22305. https://doi.org/10.1038/s41598-020-76125-y.

[2] S. Madhu & R. K. Gaur, "Effect of variable viscosity on chemically reacting magneto-blood flow with heat and mass transfer", Global Journal of Pure and Applied Mathematics **13** (2017) 26. https://doi.org/10.5890-JAND.2023.03.006.aspx.

[3] J. C. Misra, A. Sinha & G. C. Shit, "A numerical model for magnetohydrodynamic flow of blood in a porous channel", Journal of Mechanics in Medicine and Biology **11** (2011) 547. https://doi.org/10.1007/s00231-012-1107-6.

[4] L. Shu, "Numerical simulation of groundwater", Hohai University Lecture Notes, 2020. [Online]. Retrieved from https://www.iahr.org.

[5] D. S. Igba & D. A. Otor, "Simulation of Earth planetary orbits using a modified inverse square model", International Journal of Recent Innovations in Academic Research **2** (2018) 23. https://zenodo.org/record/131210.

[6] S. Ahmad, M. Farooq, A. Anjum, M. Javed, M. Y. Malik & A. S. Alshomrani, "Diffusive species in MHD squeezed fluid flow through non-Darcy porous medium with viscous dissipation and joule heating", Journal of Magnetics **23** (2018) 323. https://dspace.kci.go.kr.

[7] A. Sinha, J. C. Misra & G. C. Shit, "Effect of heat transfer on unsteady MHD flow of blood in a permeable vessel in the presence of non-uniform heat source", Alexandria Engineering Journal **55** (2016) 2023. http://creativecommons.org/licenses/by-nc-nd/4.0/.

[8] B. Zigta, "Effect of thermal radiation and chemical reaction on MHD flow of blood in stretching permeable vessel", International Journal of Applied Mechanics and Engineering **25** (2020) 198. https://doi.org/10.2478/ijame-2020-0043.

[9] P. R. Sharma & G. Singh, "Effects of variable thermal conductivity, viscous dissipation on steady MHD natural convection flow of low Prandtl fluid on an inclined porous plate with Ohmic heating", Meccanica **45** (2010) 237. https://doi.org/10.1007/s11012-009-9261-7.

[10] K. M. Joseph, S. Daniel, P. Ayuba & B. G. Agaie, "Effect of chemical reaction on unsteady MHD free convective two immiscible fluids flow", Science World Journal **12** (2017) 4. https://www.ajol.info/index.php/swj/article/view/166099.

[11] B. Zigta, "Effect of MHD blood flow with velocity, thermal and concentration slip boundary layer", Engineering and Technology Research **4** (2021) 033. https://doi.org/10.15413/etr.2021.0113.

[12] B. Zigta, "Effect of thermal radiation and chemical reaction on MHD flow of blood in stretching permeable vessel", International Journal of Applied Mechanics and Engineering **25** (2020) 198. https://doi.org/10.2478/ijame-2020-0043.

[13] A. Subhas, J. V. Tawade & J. N. Shinde, "The effects of MHD flow and heat transfer for the ucm fluid over a stretching surface in presence of thermal radiation", Hindawi Publishing Corporation Advances in Mathematical Physics **64** (2012) 702681. https://doi.org/10.1155/2012/702681.

[14] P. Sreedivya, R. Y. Sunitha & R. R. Srinivasa, "Performance of nano-casson fluid on convective flow past a permeable stretching sheet: thermophoresis and brownian motion effects", Journal of Nanofluids **10** (2021) 372. https://doi.org/10.1166/jon.2021.1796.

[15] J. C. Chato, "Heat transfer to blood vessels", Journal of Biomechanical Engineering **102** (1980) 110. https://doi.org/10.1166/jon.2021.1796.